Journal of Alloys and Compounds 509 (2011) 4828–4834

Contents lists available at ScienceDirect

Journal of Alloys and Compounds

journal homepage: www.elsevier.com/locate/jallcom

Effect of partial substitution of Cr for Ni on densification behavior, microstructure evolution and mechanical properties of Ti(C,N)–Ni-based cermets

Qingqing Yang[a], Weihao Xiong[a,*], Shiqi Li[b], Jun Li[a]

[a] State Key Lab of Materials Formation and Dies & Moulds Technology, Huazhong University of Science and Technology, Wuhan 430074, PR China
[b] School of Mechanical Science & Engineering, Huazhong University of Science and Technology, Wuhan 430074, PR China

ARTICLE INFO

Article history:
Received 1 February 2010
Received in revised form 24 January 2011
Accepted 27 January 2011
Available online 23 February 2011

Keywords:
Ti(C,N)-based cermets
Sintering
Densification behavior
Microstructure evolution
Mechanical properties

ABSTRACT

Four cermets of composition TiC–10TiN–16Mo–6.5WC–0.8C–0.6Cr_3C_2–(32 – *x*)Ni–*x*Cr (*x* = 0, 3.2, 6.4 and 9.6 wt%) were prepared, to investigate the effect of the partial substitution of Cr for Ni on densification behavior, microstructure evolution and mechanical properties of Ti(C,N)–Ni-based cermets. The partial substitution of Cr for Ni decreased full densification temperature, and the higher the content of Cr additive was, the lower full densification temperature was. The partial substitution of Cr for Ni had no significant effect of the formation of Mo_2C and Ti(C,N) and the dissolution of WC, and however, it had a significant effect on the dissolution of Mo_2C. Cr in Ni-based binder phase diffused into undissolved Mo_2C to form $(Mo,Cr)_2C$ above 1000 °C at 6.4–9.6 wt% Cr additive, and a small amount of $(Mo,Cr)_2C$ did not dissolve after sintering at 1410 °C for 1 h at 9.6 wt% Cr additive. In the final microstructure, Cr content in Ni-based binder phase increased with increasing the content of Cr additive, and however, regardless of the content of Cr additive, coarse Ti(C,N) grains generally consisted of black core, white inner rim and grey outer rim, and fine Ti(C,N) grains generally consisted of white core and grey rim. The partial substitution of Cr for Ni increased hardness and decreased transverse rupture strength (TRS). Ni-based binder phase became hard with increasing the content of Cr additive, therefore resulting in the increase of hardness and the decrease of TRS. TRS was fairly low at 9.6 wt% Cr additive, which was mainly attributed hardening of Ni-based binder phase and undissolved $(Mo,Cr)_2C$.

© 2011 Elsevier B.V. All rights reserved.

1. Introduction

Ti(C,N)-based cermets belong to a class of hard and wear-resistant materials prepared by liquid phase sintering, whose hard Ti(C,N) grains are dispersed in tough metallic binder phase (usually Co-based and Ni-based). They have widely been used as cutting tools for semi-finishing and finishing of stainless steels and carbon steels [1–7]. Moreover, they are also promising materials for metal forming tools, and wear parts such as mechanical seal rings and bearings [1].

As is well known, Ti(C,N)-based cermets were initially designed to use Ni as metallic binder, because Ni is much cheaper than Co used in WC–Co cement carbides. However, TiC–TiN–Ni and Ti(C,N)–Ni cermets do not match requirements of transverse rupture strength (TRS) and fracture toughness of the cutting tasks. This is attributed to poor wetting of Ni on TiC and Ti(C,N) particles, which results in Ti(C,N) grain coarsening and high residual porosity. For the practical applications, Mo or/and W is indispensable for Ti(C,N)–Ni-based cermets to enhance wetting via the formation of the rim of Ti(C,N) grains and to refine Ti(C,N) grains, resulting in the improvement of mechanical properties and tribological properties [2–20]. Co is often introduced to substitute for a part or the whole of Ni as metallic binder to improve TRS and fracture toughness, due to good wetting of liquid Co on TiC and Ti(C,N) particles [2,3,13–16,20]. In addition, NbC or TaC is introduced to improve hot hardness and thermal shock resistance [2,20], and Cr_3C_2 is introduced to improve TRS, due to the increase of the plasticity of the rims of Ti(C,N) grains [21].

In most Ti(C,N)-based cermets, Ti(C,N) grains exhibit the core-rim structure, consisting of black core, and white inner rim and grey outer rim, or consisting of white core and grey rim [2,12,14,22–30]. Some studies have proposed that white inner rim is formed via solid state reactions during solid state sintering stage and grey outer rim is formed via the dissolution–reprecipitation process during liquid phase sintering and subsequent cooling stages [23,25,29,30].

When used as dry cutting tools, metal hot forming tools and high temperature wear parts, the stability of microstructure and properties of Ti(C,N)-based cermets plays a key role in determining their performance. Iyori and Yokoo found that Cr addition improved TRS, toughness, wear resistance and oxidation resistance of Ti(C,N)–Ni-based cermets at high temperature [31]. Our previous work investigated the partial substitution of Cr for Ni on high temperature oxidation behavior of Ti(C,N)–Ni-based cermets in air

* Corresponding author. Tel.: +86 27 87556247; fax: +86 27 87556247.
E-mail address: whxiong@mail.hust.edu.cn (W. Xiong).

0925-8388/$ – see front matter © 2011 Elsevier B.V. All rights reserved.
doi:10.1016/j.jallcom.2011.01.180

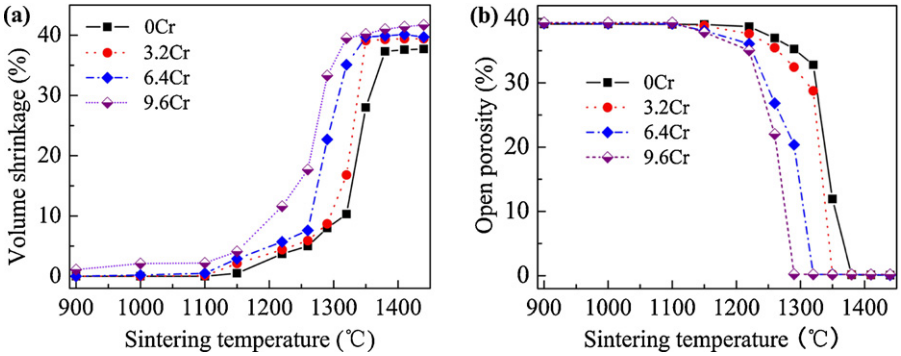

Fig. 1. Volume shrinkage (a) and open porosity (b) as a function of sintering temperature of all four experimental cermets.

[32,33]. The aim of this present paper is to investigate the effect of the partial substitution of Cr for Ni on densification behavior, microstructure evolution and mechanical properties of Ti(C,N)–Ni-based cermets.

2. Experimental procedure

Four cermets of composition TiC–10TiN–16Mo–6.5WC–0.8C–0.6Cr_3C_2–(32–*x*)Ni–*x*Cr (*x* = 0, 3.2, 6.4 and 9.6 wt%) were prepared by powder metallurgy from commercial powders of TiC (2.97 μm), TiN (7.30 μm), Mo (2.30 μm), WC (4.68 μm), C

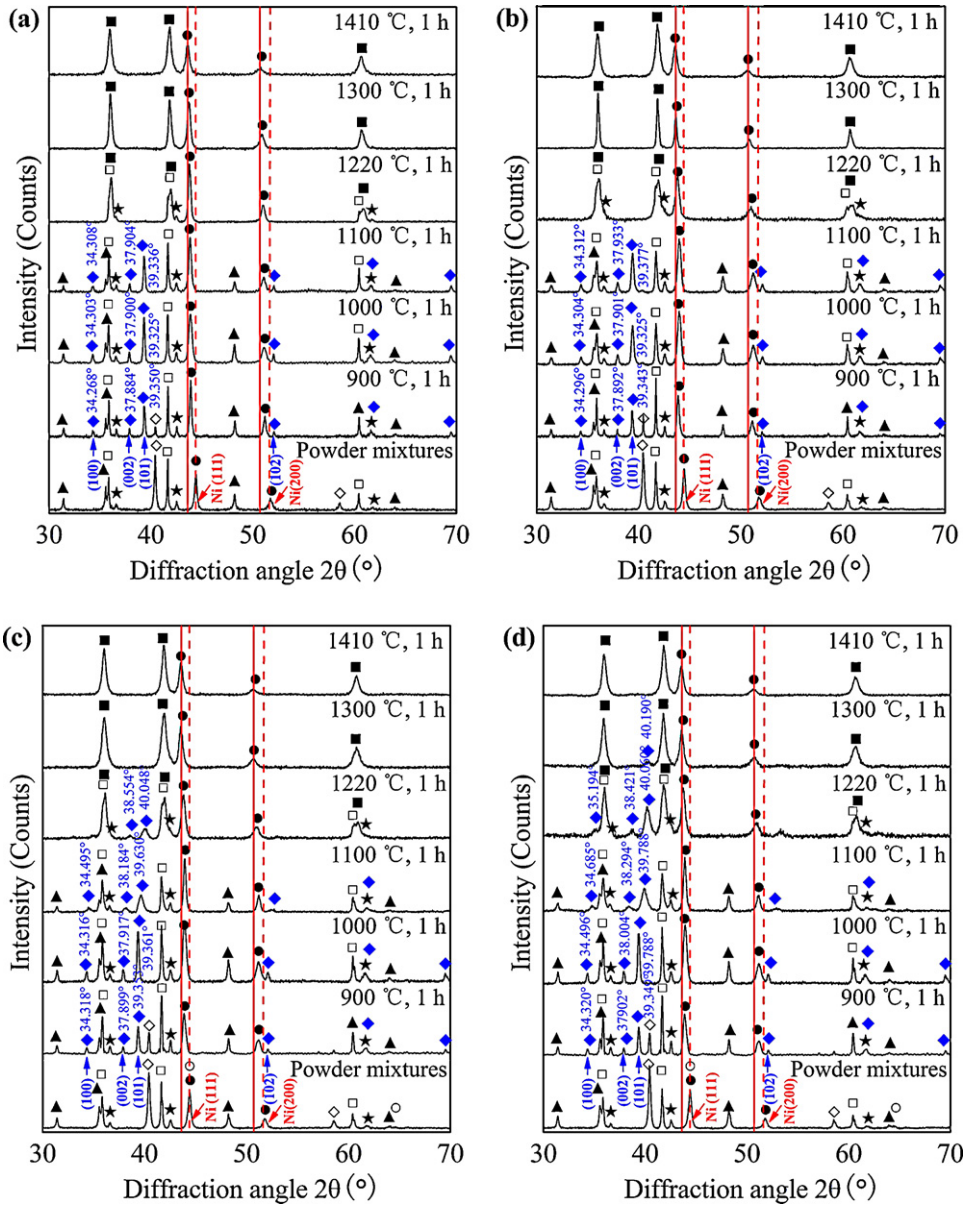

Fig. 2. XRD patterns of 0Cr (a), 3.2Cr (b), 6.4Cr (c) and 9.6Cr (d) cermets after sintering under vacuum at various temperatures for 1 h (■: Ti(C,N); □: TiC; ⋆: TiN; ▲: WC; ◊: Mo; ♦: Mo_2C; •: Ni; ○: Cr).

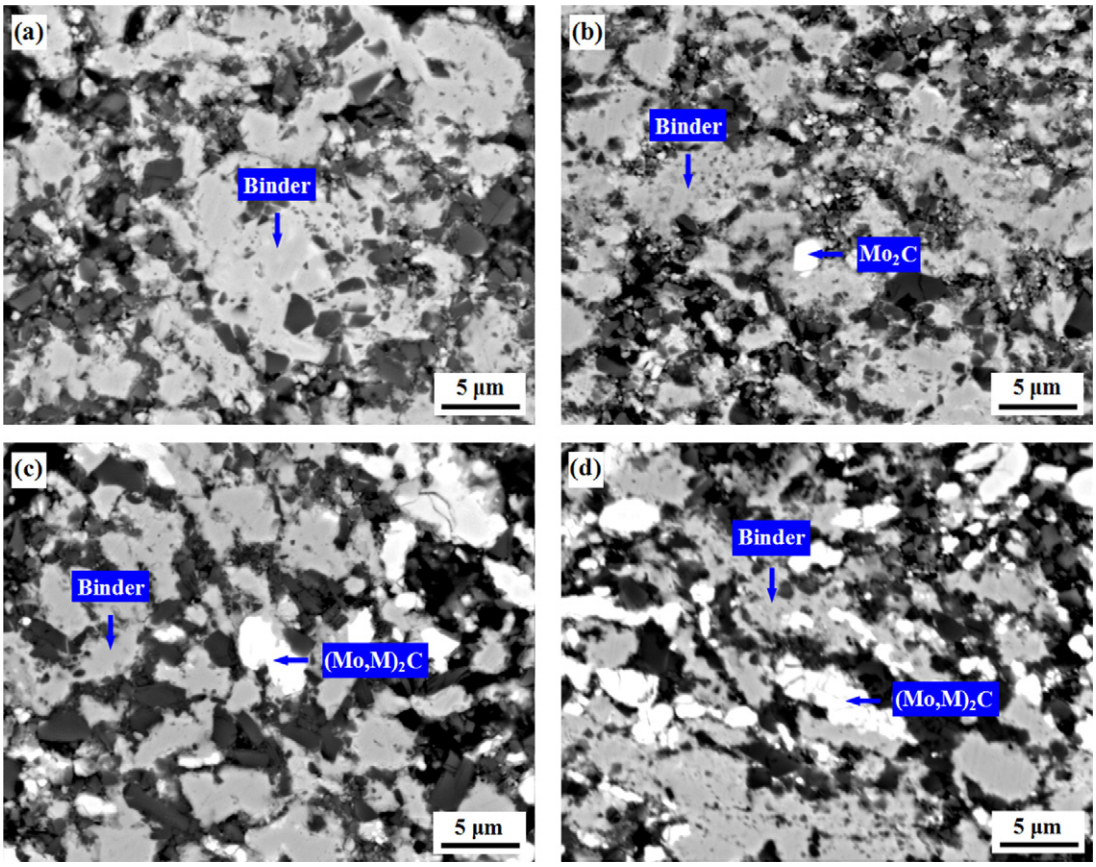

Fig. 3. SEM-BSE micrographs of polished cross-sections of 0Cr (a), 3.2Cr (b), 6.4 Cr (c) and 9.6Cr (d) cermets after sintering under vacuum at 1220 °C for 1 h.

(<30 μm), Cr_3C_2 (2.80 μm), Ni (2.25 μm) and Cr (~74 μm). For simplicity, they were also called in the following order according to the content of Cr additive: 0Cr, 3.2Cr, 6.4Cr and 9.6Cr cermets, respectively. After weighing starting powders, the powder mixtures were planetary ball-milled using WC–Co cemented carbide balls as milling balls at a ball-to-powder weight ratio of 7:1 and a speed of 200 rpm for 48 h, and then sieved and mixed with styrene butadiene polymer. Green compacts were uniaxially pressed at a pressure of 300 MPa, and then degreased under vacuum at 350–550 °C for 8 h, and sintered under vacuum at various temperatures for 1 h.

Phases were identified using X-ray diffraction (XRD, X'Pert PRO, PANalytical, Netherlands) with CuK_α radiation. Microstructure was observed using scanning electron microscopy (SEM, Quanta 200, FEI, Netherlands) in back-scattered electron (BSE) mode. Composition was analyzed using energy dispersive spectroscopy (EDS, INCA, OXFORD, UK) attached to SEM. Open porosity was measured using Archimedes method in water. Hardness and transverse rupture strength (TRS) were measured using Rockwell hardness test and three-point-bending test (the dimension of specimen 20.0 mm × 6.5 mm × 5.25 mm, span 14.5 mm), respectively.

3. Results and discussion

3.1. Densification behavior

Fig. 1 shows volume shrinkage and open porosity of all four cermets after sintering at various temperatures between 900 °C and 1440 °C for 1 h. All volume shrinkage curves in Fig. 1(a) exhibited an abrupt increase at about 1220 °C, and then reached an approximate plateau. The final volume shrinkage of 0Cr, 3.2Cr, 6.4Cr and 9.6Cr cermets was about 37.7%, 39.4%, 40.7% and 41.7%, respectively. The onset temperature of the plateau of volume shrinkage curve of 0Cr, 3.2Cr, 6.4Cr and 9.6Cr cermets was about 1380 °C, 1350 °C, 1350 °C and 1320 °C, respectively. All open porosity curves in Fig. 1(b) exhibited an abrupt decrease at about 1220 °C, and then reached

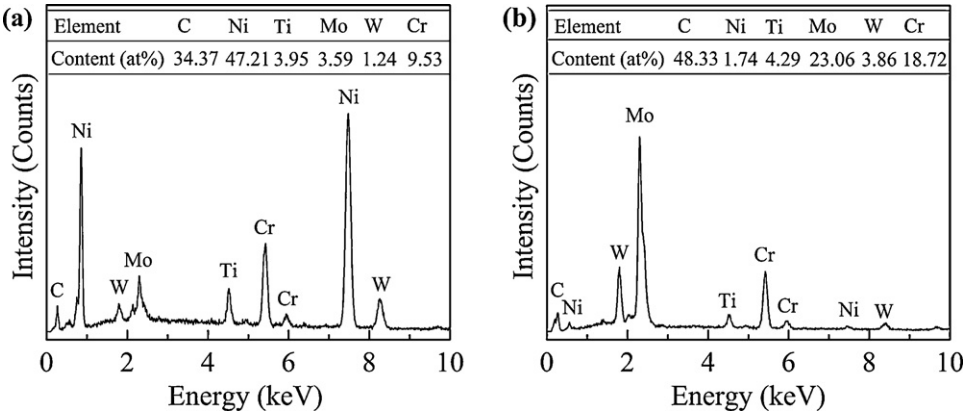

Fig. 4. SEM/EDS analysis of Ni-based binder phase (a) and $(Mo,M)_2C$ (b) of 9.6Cr cermet after sintering under vacuum at 1220 °C for 1 h.

a plateau. The final open porosity of all four cermets was close to zero. The onset temperature of the plateau of open porosity curve was about 1380 °C, 1350 °C, 1320 °C and 1290 °C for 0Cr, 3.2Cr, 6.4Cr and 9.6Cr cermets, respectively. Volume shrinkage mainly resulted from liquid pore filling [34]. These demonstrate that all four cermets were fully dense or almost fully dense at or above the onset value of plateau temperature of open porosity curves. As can be seen, the partial substitution of Cr for Ni decreased full densification temperature of Ti(C,N)–Ni-based cermets, and the higher the content of Cr additive was, the lower full densification temperature was.

3.2. Microstructure evolution

Fig. 2 shows XRD patterns of ball-milled powder mixtures and specimens sintered in vacuum at various temperatures between 900 °C and 1410 °C for 1 h of all four cermets. The diffraction peaks of Ni shifted toward low angle for all four cermets with increasing sintering temperature, that is, the lattice parameter of Ni increased with increasing sintering temperature. As can be seen, the total content of alloying elements in Ni lattice increased with increasing sintering temperature for all four cermets (atomic radii of Ni, Mo, Ti, W and Cr are 0.12458 nm, 0.13626 nm, 0.14318 nm, 0.13705 nm and 0.1249 nm, respectively). For 6.4Cr and 9.6Cr cermets, the diffraction peaks of Cr disappeared at 900 °C. This demonstrates that Cr dissolved into Ni at or below 900 °C. For all four cermets, the diffraction peaks of Mo_2C appeared at 900 °C and those of Mo disappeared at 1000 °C. These demonstrate that Mo reacted with free graphite to form Mo_2C at or below 1000 °C [23,35]. However, the relatively diffraction intensity of Mo_2C decreased at or above 1100 °C, and the diffraction peaks of Mo_2C disappeared at 1220 °C for 0Cr and 3.2Cr cermets, at 1300 °C for 6.4Cr cermet, and at 1410 °C for 9.6Cr cermet, respectively, and moreover, the diffraction peaks of Mo_2C shifted toward high angle for 6.4Cr and 9.6Cr cermets with increasing sintering temperature. These demonstrate that Mo_2C dissolved into TiC or Ti(C,N) and Ni above 1000 °C for all four cermets, and at the same time, alloying elements whose atomic radii are smaller than that of Mo diffused into undissolved Mo_2C to form $(Mo,M)_2C$ for 6.4Cr and 9.6Cr cermets, and decreased the dissolution rate of $(Mo,M)_2C$. For all four cermets, the diffraction peaks of WC disappeared about 1220 °C, and those of TiC and TiN disappeared as isolated compounds at about 1300 °C, and those of Ti(C,N) appeared about 1220 °C. These demonstrate that WC almost dissolved into TiC or Ti(C,N) and Ni at about 1220 °C, and TiC reacted with TiN to form Ti(C,N) above 1100 °C [23,35]. After sintering at 1410 °C for 1 h, the diffraction peaks of Ti(C,N) and Ni appeared for all four cermets.

Fig. 3 shows SEM-BSE micrographs of polished cross-sections of all four cermets after sintering under vacuum at 1220 °C for 1 h. There remained lots of macro-pores in all four cermets. In addition, Mo_2C in 3.2Cr cermet and $(Mo,M)_2C$ in 6.4Cr and 9.6Cr cermets did not completely dissolved, and the amount of undissolved Mo_2C or $(Mo,M)_2C$ increased in the following order: 3.2Cr < 6.4Cr < 9.6Cr. Fig. 4 shows SEM/EDS analysis of Ni-based binder phase and $(Mo,M)_2C$ in 9.6Cr cermet. The content of Cr in Ni-based binder phase was high, and those of Mo and W were relatively low. The content of Cr in $(Mo,M)_2C$ was high, and those of W and Ti were relatively low. Combined with XRD analysis in Fig. 2, $(Mo,M)_2C$ in 6.4Cr and 9.6Cr cermets was in fact $(Mo,Cr)_2C$. As can be seen, Cr in Ni-based binder phase diffused into undissolved Mo_2C to form $(Mo,Cr)_2C$ at and above 1100 °C, and decreased the dissolution rate of $(Mo,Cr)_2C$.

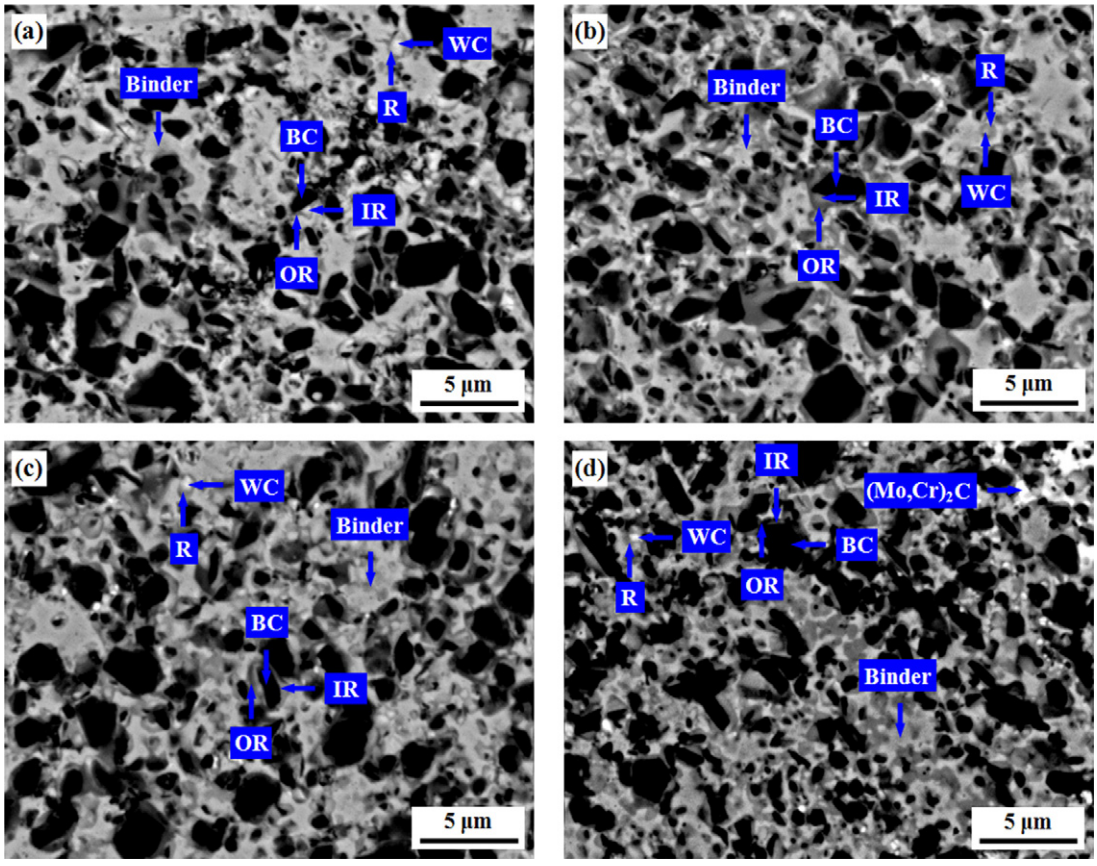

Fig. 5. SEM-BSE micrographs of polished cross-sections of 0Cr (a), 3.2Cr (b), 6.4 Cr (c) and 9.6Cr (d) cermets after sintering under vacuum at 1350 °C for 1 h (BC: black core; WC: white core; IR: white inner rim; OR: grey outer rim; R: grey rim).

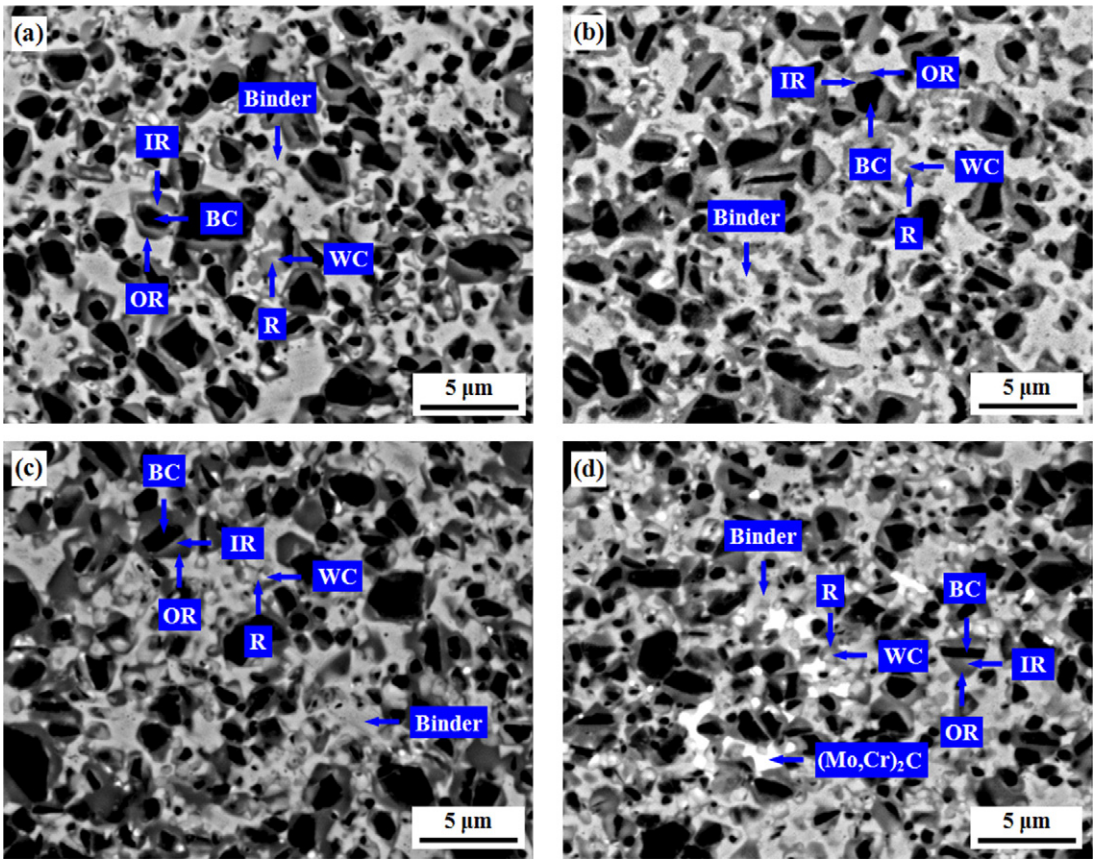

Fig. 6. SEM-BSE micrographs of polished cross-sections of 0Cr (a), 3.2Cr (b), 6.4 Cr (c) and 9.6Cr (d) cermets after sintering under vacuum at 1410 °C for 1 h (BC: black core; WC: white core; IR: white inner rim; OR: grey outer rim; R: grey rim).

Fig. 5 shows SEM-BSE micrographs of polished cross-sections of all four cermets after sintering under vacuum at 1350 °C for 1 h. 0Cr cermet was not yet dense with residual porosity, and 3.2Cr, 6.4Cr and 9.6Cr cermets were fully dense, which are in agreement with high open porosity measured using Archimedes method in Fig. 1(b). For all four cermets, in general, coarse Ti(C,N) grains consisted of black core, white inner rim and grey outer rim, and fine Ti(C,N) grains consisted of white core and grey rim.

Fig. 6 shows SEM-BSE micrographs of polished cross-sections of all four cermets after sintering under vacuum at 1410 °C for 1 h. 0Cr cermet became fully dense like the other three cermets. For all four cermets, Ti(C,N) grains were uniformly distributed in Ni-based binder phase, and grey rim or grey outer rim of Ti(C,N) grains generally became thick. In addition, a small amount of $(Mo,Cr)_2C$ did not yet dissolved in 9.6Cr cermet. Fig. 7 shows the contents of Ni, Ti, W, Mo and Cr in Ni-based binder phase of all four cermets measured by SEM/EDS analysis, without considering the contents of C and N due to the detection limit of the instrument. The content of Ni in Ni-based binder phase exhibited an approximately linear decrease, and that of Cr exhibited an approximately linear increase, and that of Ti slightly changed, and those of Mo and W basically kept constant, with increasing the content of Cr additive.

In SEM-BSE mode, microstructure containing heavy elements is shown in white. Therefore, white cores and white inner rims were richer in Mo or/and W than black cores, and grey outer rims, respectively. During solid state sintering stage, Mo and W diffused into the surface of coarse TiC or Ti(C,N) particles, and into the core of fine TiC or Ti(C,N) particles [25]. During subsequent liquid phase sintering stage, the dissolution rate of TiC or Ti(C,N) particles was significantly affected by the particle size, and fine TiC or Ti(C,N) particles fast dissolved [17]. Therefore, in the final microstructure, the surface and the core of undissolved coarse TiC or Ti(C,N) particles became white inner rims and black cores, respectively, and undissolved fine TiC or Ti(C,N) particles became white cores. Grey outer rim and grey rim formed via selective dissolution–reprecipitation process during liquid phase sintering and subsequent cooling stages [17,23,25,29,30].

3.3. Mechanical properties

Fig. 8 shows hardness and TRS at room temperature of all four cermets after sintering at various temperatures between 1250 °C

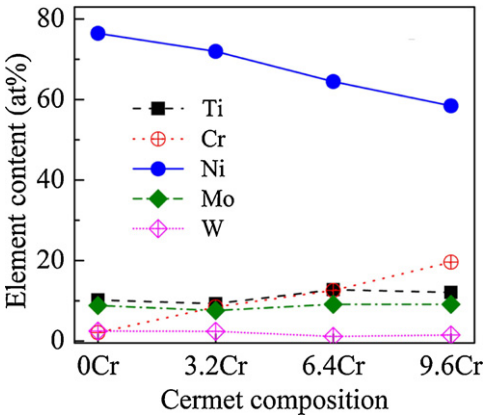

Fig. 7. The contents of Ti, W, Mo, Ni and Cr elements measured by SEM/EDS analysis in Ni-based binder phase as a function of the content of Cr additive in cermets after sintering under vacuum at 1410 °C for 1 h, without considering those of C and N.

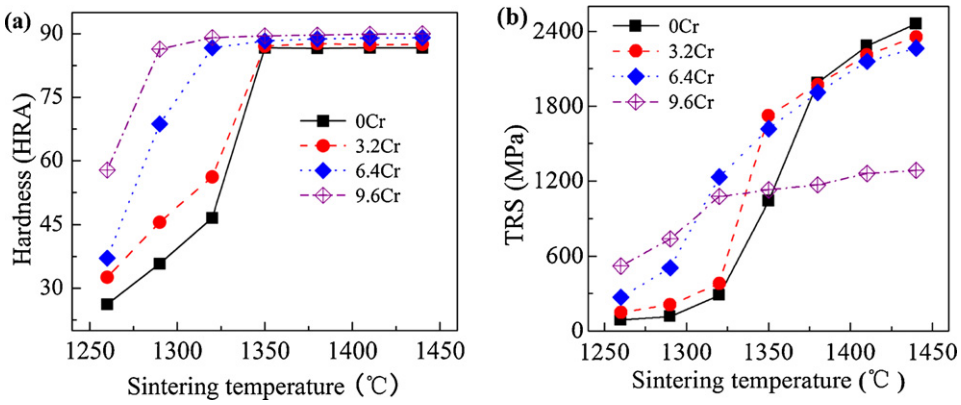

Fig. 8. Hardness (a) and TRS (b) as a function of sintering temperature of 0Cr, 3.2Cr, 6.4Cr and 9.6Cr cermets.

and 1440 °C for 1 h. It can be seen from Fig. 8 that both hardness and TRS of all four cermets were significantly affected by sintering temperature. Hardness of all four cermets was low and increased with increasing sintering temperature before full densification, and was close to a constant after full densification (Fig. 1(b)). TRS of 0Cr, 3.2Cr and 6.4Cr cermets fast increased while that of 9.6Cr cermet slow increased with increasing sintering temperature. After sintering at 1410 °C for 1 h, hardness of 0Cr, 3.2Cr, 6.4Cr and 9.6Cr cermets was 86.7 HRA, 87.7 HRA, 89.0 HRA and 89.9 HRA, respectively, and TRS was 2283 MPa, 2210 MPa, 2158 MPa and 1259 MPa, respectively. That is, the partial substitution of Cr for Ni in Ti(C,N)–Ni-based cermets increased hardness and decreased TRS.

The total content of such alloying elements as Ti, W, Mo and Cr in Ni-based binder phase increased with increasing the content of Cr additive (Fig. 7). Due to the synergistic effect of these alloying elements, Ni-based binder phase became hard, thus resulting in the increase of hardness and the decrease of TRS. TRS of 9.6Cr cermet was much lower than those of the other three cermets, which was mainly attributed hardening of Ni-based binder phase and a small amount of undissolved $(Mo,Cr)_2C$. As can be seen, for the practical applications, it is necessary for Ti(C,N)–Ni-based cermets to adjust the content of Cr additive.

4. Conclusions

TiC–10TiN–16Mo–6.5WC–0.8C–0.6Cr_3C_2–(32 − x)Ni–xCr (x = 0, 3.2, 6.4 and 9.6 wt%) cermets were prepared by powder metallurgy, in order to investigate the effect of partial substitution of Cr for Ni on densification behavior, microstructure evolution and mechanical properties of Ti(C,N)–Ni-based cermets was investigated. The following conclusions can be drawn:

1. The partial substitution of Cr for Ni decreased full densification temperature of Ti(C,N)–Ni-based cermets. Full densification temperature decreased with increasing the content of Cr additive, at least up to 9.6 wt%.
2. The partial substitution of Cr for Ni had no significant effect of the formation of Mo_2C and Ti(C,N) and the dissolution of WC, and however, it had a significant effect on the dissolution of Mo_2C. Cr in Ni-based binder phase diffused into undissolved Mo_2C to form $(Mo,Cr)_2C$ above 1000 °C at 6.4–9.6 wt% Cr additive, and a small amount of $(Mo,Cr)_2C$ did not dissolve after liquid phase sintering at 1410 °C for 1 h at 9.6 wt% Cr additive. In the final microstructure, Cr content in Ni-based binder phase increased with increasing the content of Cr additive, and however, regardless of the content of Cr additive, coarse Ti(C,N) grains generally consisted of black core, white inner rim and grey outer rim, and fine Ti(C,N) grains generally consisted of white core and grey rim. White inner rim and white core formed via the diffusion of Mo and W into TiC or Ti(C,N) particles during solid phase sintering stage, and grey outer rim and grey rim formed via selective dissolution–reprecipitation process during liquid phase sintering and subsequent cooling stages.
3. The partial substitution of Cr for Ni increased hardness and decreased transverse rupture strength (TRS). Ni-based binder phase became hard with increasing the content of Cr additive, therefore resulting in the increase of hardness and the decrease of TRS. TRS was fairly low at 9.6 wt% Cr additive, which was mainly attributed hardening of Ni-based binder phase and a small amount of undissolved $(Mo,Cr)_2C$.

Acknowledgements

This work was funded by National Science and Technology Major Project under Grant No. 2009ZX04012-022, Natural Science Foundation of Hubei Province under Grant No. 2008CDB275 and Self-researching Projects of State Key Lab of Materials Formation and Moulds & Dies Technology under Grant No. 2010-5. The authors would like to thank Analytical and Testing Center at Huazhong University of Science and Technology for providing experimental facilities.

References

[1] E.B. Clark, B. Roebuck, Int. J. Refract. Met. Hard Mater. 11 (1992) 23.
[2] P. Ettmayer, H. Kolaska, W. Lengauer, K. Dreyer, Int. J. Refract. Met. Hard Mater. 13 (1995) 343.
[3] V.R. DiZaji, M. Rahmani, M.F. Sani, Z. Nemati, J. Akbari, Int. J. Mach. Tools Manuf. 47 (2007) 768.
[4] S. Cardinal, A. Malchère, V. Garnier, G. Fantozzi, Int. J. Refract. Met. Hard Mater. 27 (2009) 521.
[5] B.V. Manoj Kumar, J. Ram Kumar, B. Basu, Int. J. Refract. Met. Hard Mater. 25 (2007) 392.
[6] W.T. Kwon, J.S. Park, S.-W. Kim, S. Kang, Int. J. Mach. Tools Manuf. 44 (2004) 341.
[7] N. Liu, S. Chao, H.D. Yang, Int. J. Refract. Met. Hard Mater. 24 (2006) 445.
[8] W.H. Xiong, Z.H. Hu, K. Cui, Acta Metall. Sin. (Chin. Lett.) 33 (5) (1997) 473.
[9] S.Q. Zhou, W. Zhao, W.H. Xiong, Y.N. Zhou, Acta Metall. Sin. (Engl. Lett.) 21 (2008) 211.
[10] K. Okuyama, T. Sakuma, Mater. Sci. Eng. A 194 (1995) 63.
[11] J. Jung, S. Kang, Acta Mater. 52 (2004) 1379–1386.
[12] S.Y. Ahn, S.-W. Kim, S. Kang, J. Am. Ceram. Soc. 84 (2001) 843.
[13] B. Vicenzi, L. Risso, R. Calzavarini, Int. J. Refract. Met. Hard Mater. 19 (2001) 11.
[14] D. Mari, S. Bolognini, G. Feusier, T. Cutard, C. Verdon, T. Viatte, W. Benoit, Int. J. Refract. Met. Hard Mater. 21 (2003) 37.
[15] E. Ehira, A. Egami, Int. J. Refract. Met. Hard Mater. 13 (1995) 313.
[16] S. Bolognini, G. Feusier, D. Mari, T. Viatte, Benoit W.F W., Int. J. Refract. Met. Hard Mater. 16 (1998) 257.
[17] Y. Zheng, W.H. Xiong, Rare Metals 20 (2001) 47.
[18] S. Park, S. Kang, Scr. Mater. 52 (2005) 129.
[19] E.T. Jeon, J. Joardar, S. Kang, Int. J. Refract. Met. Hard Mater. 20 (2002) 207.
[20] U. Rolander, G. Weinl, M. Zwinkel, Int. J. Refract. Met. Hard Mater. 19 (2001) 325.

[21] Y. Zheng, M. You, W.H. Xiong, W.J. Liu, S.X. Wang, J. Am. Ceram. Soc. 87 (3) (2004) 460.
[22] S.-Y. Ahn, S. Kang, J. Am. Ceram. Soc. 83 (2000) 1489.
[23] Y. Zheng, W.H. Xiong, M. You, W.J. Liu, Trans. Nonferrous Met. Soc. China 13 (6) (2003) 1424.
[24] J.K. Yang, H.-C. Lee, Mater. Sci. Eng. A 209 (1996) 213.
[25] N. Liu, W.H. Yin, L.W. Zhu, Mater. Sci. Eng. A 445–446 (2007) 707.
[26] Y. Zheng, W.H. Xiong, W.J. Liu, W. Lei, Q. Yuan, Ceram. Int. 31 (2005) 165.
[27] J. Qu, W.H. Xiong, D.M. Ye, Z.H. Yao, W.J. Liu, S.J. Lin, Int. J. Refract. Met. Hard Mater. 28 (2010) 243.
[28] J. Zackrisson, H.-O. Andrén, Int. J. Refract. Met. Hard Mater. 17 (1999) 265.
[29] P. Lindahl, A.E. Rosén, P. Gustafson, U. Rolander, H.-O. Andrén, Int. J. Refract. Met. Hard Mater. 8 (2000) 273.
[30] P. Lindahl, P. Gustafson, U. Rolabder, H.-O. Andrén, Int. J. Refract. Met. Hard Mater. 17 (1999) 411.
[31] Y. Iyori, H. Yokoo, US Patent 4,983,212, Jan. 8, (1991).
[32] Q.Q. Yang, W.H. Xiong, S.Q. Li, Z.H. Yao, X. Chen, Corros. Sci. 52 (10) (2010) 3205.
[33] Q.Q. Yang, W.H. Xiong, S.Q. Li, H.X. Dai, J. Li, J. Alloys Compd. 506 (1) (2010) 461.
[34] S.-J.L. Kang, K.-H. Kim, D.N. Yoon, J. Am. Ceram. Soc. 74 (2) (1991) 425.
[35] H. Yoshimura, T. Sugizawa, K. Nishigaki, Int. J. Refract. Met. Hard Mater. 1 (1983) 170.